J Wood Sci (2005) 51:448–454
DOI 10.1007/s10086-004-0681-8

ORIGINAL ARTICLE

Masato Yoshida · Daiji Fujiwara · Yukiko Tsuji
Kazuhiko Fukushima · Teruko Nakamura
Takashi Okuyama

Ultraviolet microspectrophotometric investigation of the distribution of lignin in *Prunus jamasakura* differentiated on a three-dimensional clinostat

Received: April 20, 2004 / Accepted: September 27, 2004

Abstract To examine the effect of gravity on lignin content and deposition in plant cells, we used ultraviolet (UV) microspectrophotometry and chemical methods to investigate the secondary xylem of *Prunus jamasakura* grown on a three-dimensional (3D) clinostat, which simulates microgravity. The stem of the 3D-clinostat specimens elongated with bending and the width of their secondary phloem increased. The UV absorbance of the 3D-clinostat specimens at 278 nm was higher than that of the control specimens, which were grown on the ground, in the wood fiber cell corner middle lamella, compound middle lamella, and fiber secondary wall; the UV absorbance in the vessel secondary wall did not differ between the specimens. The lignin content in the stem, including the bark, of the 3D-clinostat specimens, as determined using an acetyl bromide method, was less than that of the control specimens. In the specimens that differentiated on a 3D clinostat, the amount of lignin in the wood fibers increased, while the proportion of the lignified xylem in the stem decreased relative to control values.

Key words 3D-clinostat · Lignin distribution · UV microspectrophotometry · Microgravity

Introduction

Lignin is one of the major components of the plant cell wall; it hardens the cell wall by cementing wood fibers together. Lignin deposition starts in the cell corner middle lamella (CCML). After the middle layer of the secondary wall (SW) begins to thicken, lignin deposition spreads to the compound middle lamella (CML) and the SW. The lignin concentration is high in the CML and low in the SW. The amount of lignin changes in hypergravity and microgravity environments. The amount of lignin in the hypocotyls of cress grown under hypergravity increases,[1] while it decreases in plants grown under microgravity (in space).[2]

Lignin in the fiber secondary wall (FSW) affects its mechanical function of supporting the plant body.[3] Lignin is embedded in a polysaccharide matrix, giving rigidity and cohesiveness to wood tissue as a whole.[3] Lignin in the FSW provides rigidity, while lignin in the CML and CCML gives cohesiveness to wood tissue. Consequently, we expect that differences in the cell wall lignin of specimens that differentiate in different gravity environments would arise mainly in the FSW. To examine this, we investigated the secondary xylem of plants that differentiated in a three-dimensional (3D) clinostat, which simulates microgravity.

A 3D clinostat has two rotation axes placed at right angles. Rotation is achieved using two computer-controlled motors and is monitored by encoders attached to the motors. Rotating plants in three dimensions at random rates on a 3D clinostat alters the effect of gravity on morphogenesis, making a 3D clinostat a valuable device for simulating weightlessness.[4] Only a few studies have examined woody plants that have differentiated on a 3D clinostat. Nakamura et al.[5] found that in 3D-clinostat specimens of *Prunus jamasakura*, the stems were longer, the secondary xylem was thinner, the vessels were denser, and the microfibril angle was greater, and the stem elongated with bending, which are traits that have also been observed in plants grown in space.[2]

This study analyzed the lignin in the stem and the microdistribution of lignin in the cell walls of *Prunus jamasakura* that differentiated on a 3D clinostat and on the ground. Acetyl bromide digestion, thioacidolysis, and ultraviolet (UV) microspectrophotometry were used to characterize the lignin in the wood fiber CCML, CML, FSW, and vessel secondary wall (VSW).

M. Yoshida (✉) · D. Fujiwara · Y. Tsuji · K. Fukushima · T. Okuyama
Graduate School of Bioagricultural Sciences, Nagoya University, Nagoya 464-8601, Japan
Tel. +81-52-789-4153; Fax +81-52-789-4150
e-mail: yoshida@agr.nagoya-u.ac.jp

T. Nakamura
Faculty of Science, Japan Women's University, Tokyo 112-8681, Japan

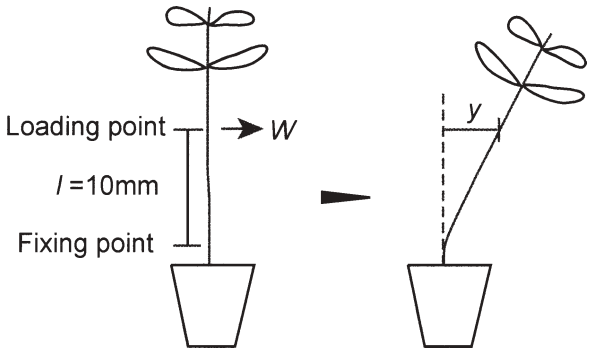

Fig. 1. Measuring the bending rigidity using cantilever beam theory. The distance from the *fixing point* to the *loading point* (l) was 10 mm. The loaded value (W) and displacement (y) at the loading point were measured under the proportional limit

Materials and methods

Plant materials

Two *Prunus jamasakura* Siebold ex Koidz. seedlings were germinated and grown on a 3D clinostat for 1 month, and two seedlings were germinated in the ground in a growth cabinet with automatically controlled temperature and humidity (temperature 22° ± 1°C; humidity 70% ± 5%). The light period was set at 12.5 h of light and 11.5 h of darkness, with a light flux of about 70 μmol mm^{-2} s^{-1}. For more details, see Nakamura et al.[5]

True compensation for the effect of the gravity vector can be achieved with the 3D clinostat when the rotation rates of the two motors are changed randomly at regular intervals, from 1 to −1 (reverse direction) rpm every 30 or 60 s.[4]

Bending test

The bending rigidity at the basal internode of the stem was determined using cantilever beam theory after the 1-month growth period (Fig. 1). The distance from the fixation point to the loading point (l) was 10 mm. The loaded value (W) and displacement (y) at the loading point were measured under the proportional limit. The bending rigidity (EI) was calculated using the formula:

$$y = \frac{l^3}{3EI}W$$

where E is the modulus of longitudinal elasticity, and I is the moment of inertia of area.

Improved acetyl bromide method

The 3D-clinostat and control stems, including bark, were dried at 105°C and cut into approximately 60-mesh pieces. Samples (10 mg each) were placed in four glass reaction bottles (35 ml) with 25% (w/w) acetyl bromide in acetic acid (10 ml) and perchloric acid (70%, 0.4 ml). The bottles were sealed with polytetrafluoroethylene-coated silicone caps, placed in an oven at 70° ± 0.2°C for 30–120 min, and shaken gently at 10-min intervals. After digestion, the solution was transferred to a 100-ml volumetric flask containing 2 M sodium hydroxide (20 ml). The sample bottle was rinsed, and the solution was diluted to 100 ml with acetic acid. The UV absorption spectrum of the solution was measured by UV spectrophotometry against a blank solution, which was run in conjunction with the sample. The lignin content was determined by measuring the absorbance at 280 nm and using a lignin absorptivity of 20.0 cm^{-1} l g^{-1}.[6]

Thioacidolysis of lignin

Thioacidolysis was carried using the method of Rolando et al.[7] with some modifications. A mixture of dioxane and ethanethiol (5 ml, 8.75:1, v/v) containing 0.2 M boron trifluoride etherate was added to the wood meal (5 mg) in a test tube with a screw cap; 0.5 mg of *n*-docosane dissolved in dioxane was added as an internal standard. The test tube was sealed with a Teflon-lined screw cap. After heating at 100°C for 4 h, with occasional stirring, the reaction mixture was cooled, and the pH of the mixture was adjusted to 3–4 with aqueous 0.4 M sodium hydrogen carbonate. The whole mixture was extracted with dichloromethane (3 × 5 ml). The combined organic layers were concentrated by evaporation at 40°C after drying with anhydrous sodium sulfate. Part of the condensed solution was trimethylsilylated at room temperature with 30 μl of *N*,*O*-bis(trimethylsilyl) trifluoroacetamide (BSTFA) and 3 μl of pyridine. The silylated derivatives were subjected to gas chromatography (GC) analysis on a GC353 system (GL Sciences, Tokyo, Japan) attached to a flame ionization detector (280°C), a solvent cut-injector (250°C), and a fused silica capillary column (TC1, 60 m × 0.25 mm i.d.). The carrier gas was nitrogen and the temperature was programmed to increase at 2°C/min from 180°C to 280°C, where it was held for 20 min. The degraded products were quantified using the value of 1.5 as a response factor.

Microscopy

Five-millimeter-long segments were obtained from the basal internode, fixed with 3% glutaraldehyde, and were embedded in epoxy resin.

For light microscopy, 2-μm-thick cross sections were cut with a glass knife and stained with 3% toluidine blue in water for 1 h. After staining, the cross sections were mounted on glass slides with Entellan (Merck, Germany) as the mounting medium and covered with micro coverslips. The thin sections were observed using light microscopy (Axiophot-2, Zeiss). The radial and tangential diameters and the thickness of at least 20 different wood fibers and vessels were measured with an image analyzer with an accuracy of 0.25 μm (KS-400, Zeiss). Extremely small wood fibers and vessels were excluded from the measurements.

The thickness of the wood fiber cell walls was measured at the midpoint.

For UV microscopy, 1-μm-thick cross sections were cut with a glass knife, mounted on quartz microscope slides, immersed under a drop of non-UV-absorbing glycerin, and covered with a quartz coverslip. The thin sections were observed under a microspectrophotometer (MPM800, Zeiss). UV absorption spectra of the mature wood fiber CCML, CML, FSW, and VSW were obtained for wavelengths of 250–350 nm using the smallest measuring spot available with the microspectrophotometer (0.5 μm diameter). Measurements were made for at least 50 different positions and averaged to determine the UV absorption spectra. The microspectrophotometer settings were: objective lens magnification: ×100, program: Lambdascan, bandwidth: 1 nm, scan step: 1 nm, and number of scans: 45. The thickness of each thin section was measured with an accuracy of 0.01 μm using a universal surface shape profiler (SE-3E, Kosaka), in order to select sections with uniform thickness and to correct the UV absorption spectra.[8] For more details, see Scott and Goring[9] and Gindl and Okuyama.[10]

To estimate the changes in the ratio of syringyl lignin (S) to guaiacyl lignin (G) (S/G ratio) in the FSW, CML, CCML, and VSW of specimens, the ratios of the absorption at 280 nm to that at 273 nm (A_{280}/A_{273}) and the absorption at 280 nm to that at 260 nm (A_{280}/A_{260}), as well as the absorption maxima (λ_{max}), were calculated for the 3D-clinostat and control specimens.[11–16]

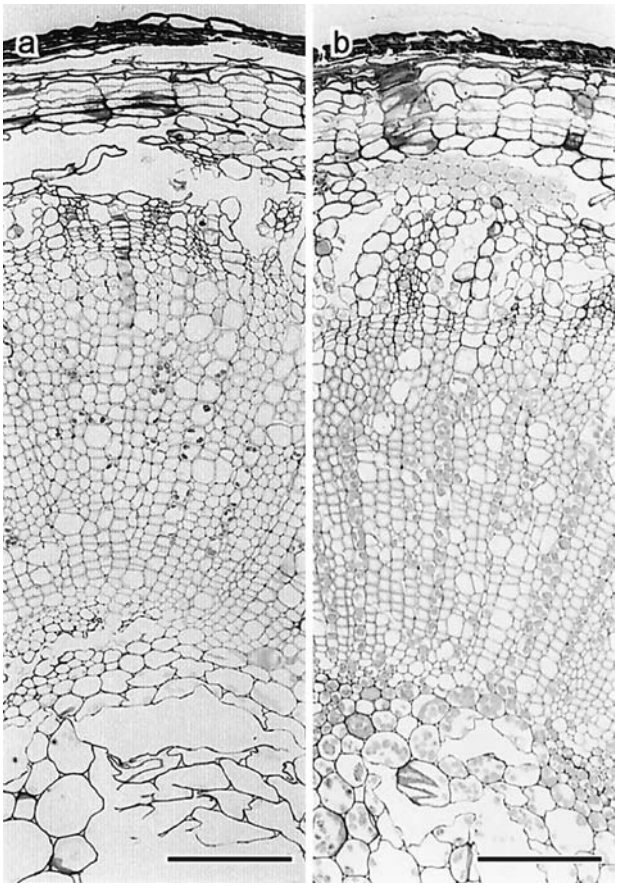

Fig. 2. Light micrographs of cross-sections of the 3D-clinostat specimen (**a**) and the control specimen (**b**). *Bars* 100 μm

Results

Plant appearance and bending rigidity

The stems of the 3D-clinostat specimens elongated with bending, while the stems of the controls remained straight. The stems of the 3D-clinostat specimens were longer than those of the controls (121 and 132 mm vs 107 and 132 mm, respectively). The diameters of the 3D-clinostat specimens were larger than those of the controls (1.6 and 1.3 mm vs 1.25 and 1.25 mm, respectively). The bending rigidities of the 3D-clinostat specimens were greater than those of the controls (7.3×10^3 and 4.2×10^3 g mm^2 vs 3.0×10^3 and 2.7×10^3 g mm^2, respectively). These results indicate that the 3D-clinostat specimens were more difficult to bend.

Lignin in the stem

The average lignin content of the 3D-clinostat specimen was less than that of the controls (6.28% ± 0.61% vs 7.98% ± 0.27%, respectively; $n = 4$; $P < 0.01$). The S/G ratio determined by thioacidolysis did not differ significantly between the 3D-clinostat (1.87) and control specimens (1.88).

Light microscopy

Eccentric growth was not observed in the 3D-clinostat or control specimens. Figure 2 shows light micrographs of cross sections of the 3D-clinostat (a) and control (b) specimens. The bark of the 3D-clinostat specimens was slightly thicker than that of the controls (220 ± 30 μm vs 170 ± 22 μm, respectively; $P = 0.32$). The secondary xylem, excluding the pith, of the 3D-clinostat and control specimens had roughly the same width (280 ± 9 μm vs 280 ± 23 μm, respectively; $P = 0.97$). The vessels were denser in the secondary xylem of the 3D-clinostat specimens than in the controls (490 ± 7/mm^2 vs 410 ± 11/mm^2, respectively; $P < 0.01$). The diameter of the wood fibers and wood fiber cell wall thickness of the 3D-clinostat specimens were larger than those of controls (Table 1). The vessel diameters and vessel cell wall thicknesses of the 3D-clinostat and control specimens did not differ.

UV microscopy

Figure 3 shows UV micrographs and absorption profiles across the cell walls of wood fibers of the 3D-clinostat (a) and control (b) specimens at a wavelength of 278 nm. The

Table 1. The radial and tangential diameters and thickness of wood fibers, and the vessel diameter and thickness

	Diameter (μm)			Thickness (μm)		
	Radial**	Tangential**	Vessel[a]	Radial*	Tangential***	Vessel[a]
3D clinostat	9.1 (0.8)	11.5 (1.0)	15.5 (2.4)	2.0 (0.2)	2.2 (0.2)	0.8 (0.2)
Control	8.6 (0.8)	11.0 (0.8)	14.7 (2.6)	1.9 (0.2)	2.0 (0.2)	0.8 (0.1)

All values are expressed as the mean (standard deviation) of two individuals
* $P < 0.05$, ** $P < 0.01$, *** $P < 0.001$
[a]Not significant by the *t*-test

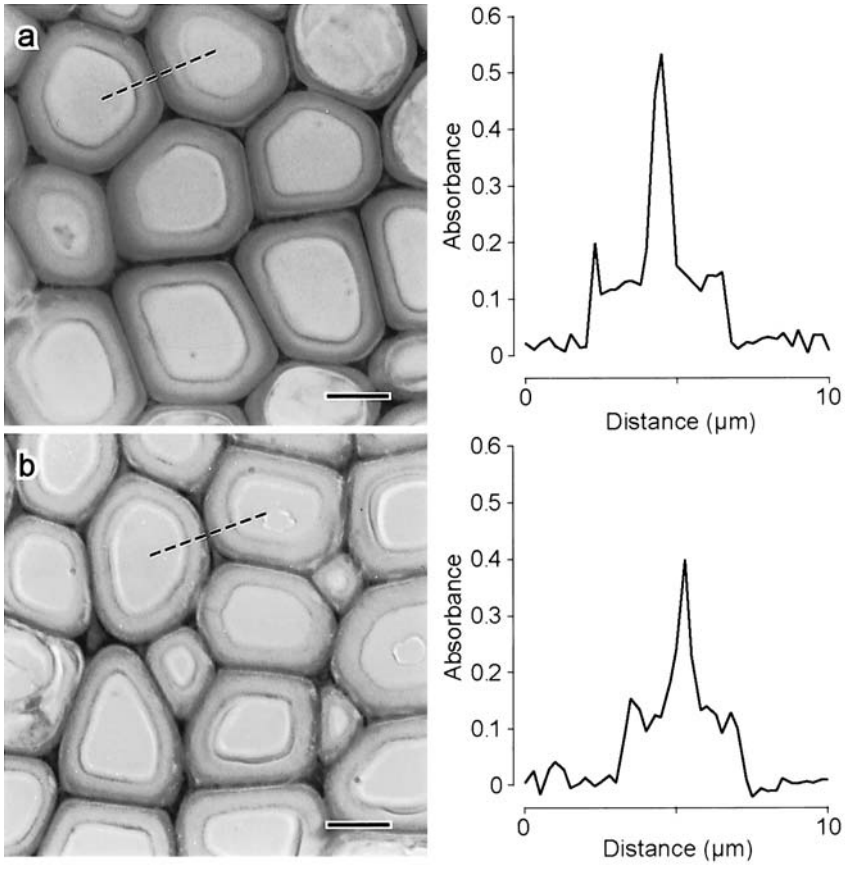

Fig. 3. Ultraviolet (UV) micrographs of cross-sectionalprofiles and absorption profiles across the cell walls of wood fibers at 278 nm for the 3D-clinostat specimen (**a**) and the control specimen (**b**). The *dotted lines* indicate the positions of the absorption profiles. The radial direction is vertical. *Bars* 5 μm

UV absorbance was high in the CCML and CML and low in the FSW. The UV absorbance of the FSW indicated that it was not a gelatinous layer.

The UV absorbance of the 3D-clinostat specimens was higher than that of the control specimens in every part. In the FSW of the 3D-clinostat specimens, the outer layer had a higher UV absorbance than the inner layer. Nevertheless, in the line scan measurement of the 3D-clinostat specimens, the higher UV absorbance of the outer layer and the lower UV absorbance of the inner layer were not confirmed. Moreover, the UV absorption spectra of the outer and inner layers of the FSW did not differ significantly, so that in Fig. 4, the UV absorption in the center of the FSW is shown.

The UV absorbance was highest in the CCML and decreased in the CML and FSW, in that order (Fig. 4). The absorbance of the wood fibers of the 3D-clinostat specimens was higher than that of the controls at all spots measured, while the absorbance of the VSW did not differ between the specimens.

For the 3D-clinostat specimens, the average UV absorbance at 278 nm was 1.1 times the control value in the FSW ($P < 0.01$), 1.4 times the control value in the CML ($P < 0.01$), and 1.2 times the control value in the CCML ($P < 0.05$) (Table 2). The absorption maxima (λ_{max}) of the 3D-clinostat and the control specimens ranged from 277 to 279 nm. While the λ_{max} of the CCML, FSW, and VSW did not differ significantly between the specimens, the λ_{max} of the CML was shifted to a wavelength that was 2 nm longer in the 3D-clinostat specimens relative to the control specimens ($P < 0.05$).

The A_{280}/A_{273} and A_{280}/A_{260} absorbance ratios are tabulated in Table 3. Neither ratio differed significantly in the

Table 2. Absorbance at 278 nm and absorption maxima (λ_{max}) in regions of the cell walls of wood fibers and vessels of 3D-clinostat and control samples

	Absorbance				λ_{max} (nm)			
	CCML*	CML**	FSW**	VSW[a]	CCML[a]	CML**	FSW[a]	VSW[a]
3D clinostat	0.61 (0.06)	0.52 (0.05)	0.13 (0.01)	0.34 (0.02)	278 (1.3)	279 (0.5)	279 (1.2)	278 (0.3)
Control	0.53 (0.06)	0.37 (0.01)	0.11 (0.01)	0.34 (0.02)	278 (0.8)	277 (1.1)	279 (1.5)	279 (0.3)

All values are expressed as the mean (standard deviation) of two individuals
CCML, wood fiber cell corner middle lamella; CML, wood fiber compound middle lamella; FSW, wood fiber secondary wall; VSW, vessel secondary wall
* $P < 0.05$, ** $P < 0.01$
[a] Not significant by *t*-test

Table 3. Ratios of the absorbance at 280 nm to that at 273 nm (A_{280}/A_{273}) and the absorbance at 280 nm to that at 260 nm (A_{280}/A_{260})

	A_{280}/A_{273}				A_{280}/A_{260}			
	CCML[a]	CML[a]	FSW[a]	VSW[a]	CCML[a]	CML[a]	FSW[a]	VSW[a]
3D clinostat	1.04 (0.02)	1.04 (0.03)	1.03 (0.03)	1.04 (0.002)	1.29 (0.11)	1.22 (0.03)	1.23 (0.06)	1.25 (0.03)
Control	1.03 (0.03)	1.03 (0.01)	1.06 (0.02)	1.03 (0.002)	1.21 (0.06)	1.24 (0.03)	1.24 (0.06)	1.26 (0.02)

All values are expressed as the mean (standard deviation) of two individuals
[a] Not significant by the *t*-test

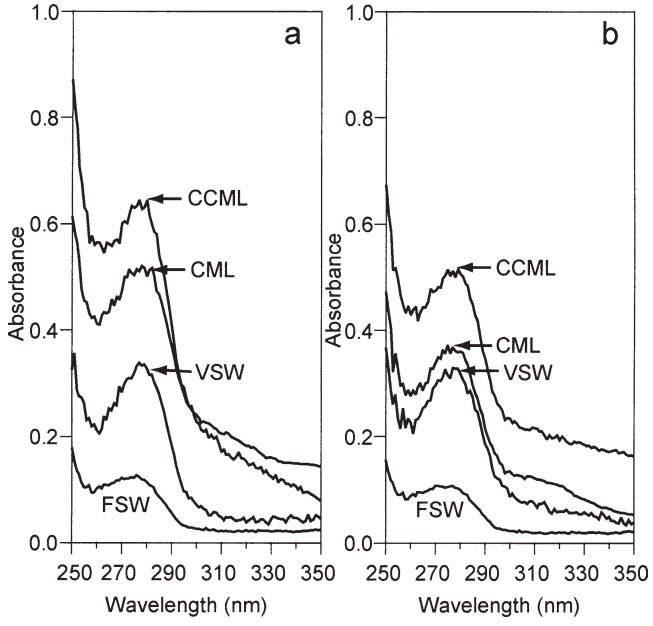

Fig. 4. UV absorption spectra of the cell corner middle lamella (*CCML*), compound middle lamella (*CML*), and secondary wall of wood fibers (*FSW*), and the vessel secondary wall (*VSW*) in the 3D-clinostat specimen (**a**) and the control specimen (**b**)

FSW, CML, CCML, or VSW between the 3D-clinostat and the control specimens.

Discussion

Comparison with previous studies

A 3D clinostat is a valuable device for simulating weightlessness.[4] When a plant is grown in a 3D clinostat, the gravity vector can cause changes in plant formation similar to those seen in plants grown under microgravity in space. However, some divergent results have been reported.[17] This might be because the effect of simulating microgravity using clinostats depends on the rotation frequency of the clinostat; the size, mass, and density of the gravity-susceptible organelles; and the viscosity and density of the medium surrounding the organelles.[4]

Our finding that the stems were longer and bent and the vessels were denser in 3D-clinostat specimens when compared with controls matched the findings of Nakamura et al.[5] The vessels of the 3D-clinostat specimens give preference to water transport over mechanical function under simulated microgravity conditions. Our finding that the width of the secondary xylem of 3D-clinostat specimens equaled that of the controls counters the finding of Nakamura et al.[5] that the xylem was thinner in 3D-clinostat specimens. Because only a few studies have examined woody plants, the graviresponse of woody plants grown on a 3D clinostat is still unclear. Our specimens were older than the previously studied specimens. The seedlings grew in the presence of a gravitational force oriented in random

directions on the 3D clinostat; consequently, the stem bent and various stresses were generated. These factors will influence secondary xylem differentiation.

Lignin

The lignin content of the stem, including bark, in the 3D-clinostat specimens decreased. This concurs with microgravity experiments in space.[2] In the 3D-clinostat specimens, the stem diameter and bark width were larger than in the controls, while the xylem width was the same as in the controls. Therefore, the proportion of xylem in the stem decreased in 3D-clinostat specimens. This suggests that there might be a consequent decrease in the lignin content of the stem.

We focused on the lignin distribution in the cell walls of the secondary xylem and the lignin content of the specimens that differentiated on the 3D clinostat. Lignin in the CCML and CML serves to cement cells together. The FSW makes the dominant contribution to the mechanical properties of the cell wall[3,18] and is essential for supporting the plant body.

Increasing UV absorption suggests increasing lignin content, assuming the same S/G ratio.[11,19–21] Because UV micrographs show reflected UV light, dark regions indicate areas of strong UV absorption. The 3D-clinostat specimens showed a higher lignin content than did the control specimens in the FSW, CML, and CCML, while the lignin contents in the VSW were approximately the same; the S/G ratio was the same in the 3D-clinostat specimens and the controls, as shown below.

The UV absorption of hardwood lignin in the 280-nm region depends on the ratio of syringyl propane (S) units to guaiacyl propane (G) units, but the ratio is not effective for quantifying hardwood lignin. The accurate measurement of the S/G ratio using UV spectroscopy is difficult because the λ_{max} values of the S and G units are similar (270 vs 280 nm, respectively). Moreover, S and G lignins have different UV absorptivity. However, changes in the S/G ratio can be estimated from the UV absorption spectra.[11–16] The S/G ratio increases as the λ_{max} of the spectrum decreases from 280 nm.[11,14] Decreases in the A_{280}/A_{273} and A_{280}/A_{260} ratios correspond to increases in the S/G ratio.[11–13] In our study, the λ_{max} of the CML shifted to a longer wavelength by 2 nm in the 3D-clinostat specimens, but there were no other changes in λ_{max}, A_{280}/A_{273}, or A_{280}/A_{260} in the FSW, CML, CCML, or VSW. In addition, the S/G ratio in the stem that was estimated using thioacidolysis was the same. The S/G ratio is unlikely to be changed at any of the measured spots in the 3D-clinostat specimens.

This study indicated that lignin in wood fibers increased in 3D-clinostat specimens, while the proportion of the lignified xylem decreased.

Effect of 3D clinostat conditions on tree growth

The 3D-clinostat specimens were more difficult to bend than were the control specimens. The specimens on the 3D clinostat were rotated in three dimensions, so that the gravity vector changed throughout the period of growth. The stem always bent, and bending stress was generated in it. The stimuli due to deflection and stress will increase the bending rigidity of the 3D-clinostat specimens by inducing increased lignin content, increased cell wall thickness, and increased basal internode diameter.

With trunk inclination, when the gravity vector shifts from being directed vertically downward, tension wood is formed in order to maintain posture.[22] In tension wood, the lignin content of the FSW decreases and a gelatinous layer often develops. As the 3D-clinostat specimens grew while rotating in three dimensions, they were usually inclined from the vertical during growth. However, there was no tension wood or eccentric growth in the 3D-clinostat specimens. This is because in order to develop tension wood, the gravity vector must shift from the vertical and the condition must be maintained for a certain period.

A recent study[23] found a disordered arrangement of the cells in the secondary xylem and undeveloped secondary cell wall of the bast fiber in the secondary phloem. The differentiation and development of the secondary xylem and the secondary phloem will be controlled by terrestrial gravity. In our study, changes in the lignin distribution in mature secondary xylem was investigated. Further study will observe the differentiation and development of the cell wall of the secondary xylem.

Trees have not been sent on spaceflights, so it is not known whether the results of our 3D-clinostat study are similar to those that would occur in space. Nevertheless, this study found that gravity has an effect on morphogenesis and cell wall differentiation.

References

1. Hoson T, Nishitani K, Miyamoto K, Ueda J, Kamisaka J, Yamamoto R, Masuda Y (1996) Effects of hypergravity on growth and cell wall properties of cress hypocotyls. J Exp Bot 47:513–517
2. Cowles JR, Scheld HW, LeMay R, Peterson C (1984) Growth and lignification in seedlings exposed to eight days of microgravity. Ann Bot 54:33–48
3. Plomion C, Leprovost G, Stokes A (2001) Wood formation in trees. Plant Physiol 127:1513–1523
4. Hoson T, Kamisaka S, Masuda Y, Yamashita M, Buchen B (1997) Evaluation of the three-dimensional clinostat as a simulator of weightlessness. Planta 203:S187–197
5. Nakamura T, Sassa N, Kuroiwa E, Negishi Y, Hashimoto A, Yamada M (1999) Growth of *Prunus* tree stems under simulated microgravity conditions. Adv Space Res 23:2017–2020
6. Iiyama K, Wallis AFA (1988) An improved acetyl bromide procedure for determining lignin in woods and wood pulps. Wood Sci Technol 22:271–280
7. Rolando C, Monties B, Lapierre C (1992) Thioacidolysis. In: Lin SY, Dence CW (eds) Methods in lignin chemistry. Springer, Berlin Heidelberg New York, pp 334–349
8. Okuyama T, Takeda H, Yamamoto H, Yoshida M (1998) Relation between growth stress and lignin concentration in the cell wall: ultraviolet microscopic spectral analysis. J Wood Sci 44:83–89
9. Scott JAN, Goring DAI (1970) Photolysis of wood microsections in the ultraviolet microscope. Wood Sci Technol 4:237–239
10. Gindl W, Okuyama T (1999) Increase of error in lignin measurement using ultraviolet microscopy due to multiple scanning. J Wood Sci 45:179–180

11. Fergus BJ, Goring DAI (1970) The location of guaiacyl and syringyl lignin in birch xylem tissue. Holzforschung 24:113–117
12. Musha Y, Goring DAI (1975) Distribution of syringyl and guaiacyl moieties in hardwoods as indicated by ultraviolet microscopy. Wood Sci Technol 9:45–58
13. Fujii T, Shimizu K, Yamaguchi A (1987) Enzymatic saccharification on ultrathin sections and ultraviolet spectra of Japanese hardwoods and softwoods (in Japanese). Mokuzai Gakkaishi 33: 400–407
14. Yoshinaga A, Fujita M, Saiki H (1992) Relationships between cell evolution and lignin structural varieties in oak xylem evaluated by microscopic spectrophotometry with separated cell walls (in Japanese). Mokuzai Gakkaishi 38:183–196
15. Yoshida M, Ohta H, Okuyama T (2002) Tensile growth stress and lignin distribution in the cell walls of black locust (*Robinia pseudoacacia*). J Wood Sci 48:99–105
16. Yoshida M, Ohta H, Yamamoto H, Okuyama T (2002) Tensile growth stress and lignin distribution in the cell walls of yellow poplar, *Liriodendron tulipifera* Linn. Trees 16:457–464
17. Yamashita M, Yamashita A, Yamada M (1997) Three-dimensional (3D) clinostat and its operational characteristics. Biol Sci Space 11:112–118
18. Yamamoto H, Kojima Y, Okuyama T, Abasolo WP (2002) Origin of the biomechanical properties of wood related to the fine structure of the multi-layered cell wall. Trans ASME J Biomech Eng 124:432–440
19. Fergus BJ, Goring DAI (1970) The distribution of lignin in birch wood as determined by ultraviolet microscopy. Holzforschung 24:118–124
20. Kleist G, Bauch J (2001) Cellular UV microspectrophotometric investigation of sapelli heartwood (*Entandrophragma cylindricum* Sprague) from natural provenances in Africa. Holzforschung 55: 117–122
21. Gindl W (2002) Comparing mechanical properties of normal and compression wood in Norway spruce: the role of lignin in compression parallel to the grain. Holzforschung 56:395–401
22. Nakamura T, Yoshida M (2000) Woody plant and gravity (in Japanese). Biol Sci Space 14:123–131
23. Yoneyama E, Ishimoto-Negishi Y, Sano Y, Funada R, Yamada M, Nakamura T (2004) Morphological changes in woody stem of *Prunus jamasakura* under simulated microgravity. Bio Sci Space 18:3–6